Anal. Chem. **1996,** *68,* 1095−1100

Laser-Induced Breakdown Spectrometry of Titanium Dioxide Antireflection Coatings in Photovoltaic Cells

M. Hidalgo,[†] F. Martín,[‡] and J. J. Laserna*,[†]

Department of Analytical Chemistry and Department of Chemical Engineering, Faculty of Sciences, University of Málaga, E-29071 Málaga, Spain

Silicon photovoltaic cells have design and material requirements different from those of most other silicon electronic devices. Not only are nearly ideal silicon surfaces required, but also the bulk properties must be of uniform high quality for high-energy conversion efficiency. In this paper, emission spectra of laser-generated plasmas from titanium dioxide antireflection coatings in solar cells are reported. A pulsed nitrogen laser at 337.1 nm was used with a pulse width of 10 ns and a laser fluence of 8.6 J/cm^2 onto the sample. The plasmas were detected using a charge-coupled device. Depth profilings from several samples with different thicknesses of titanium dioxide have been studied. A method for measuring thin TiO_2 films based on the observation of such profiles was developed. The effect of the laser fluence on the sensitivity of the present method has been examined. Depth resolutions are fluence-dependent but are on the order of 40 nm. The dependence between titanium dioxide plasma intensity and material reflectivity at the laser wavelength is discussed. Another valuable aspect of the technique is the ability to perform measurements in a contactless manner at room temperature and atmospheric pressure on wafer-sized samples.

Photovoltaic technology (PV) is just now maturing enough to allow reliable cost and performance estimates by utility planners. The cost of PV-generated electricity is rapidly approaching that of fossil-generated electricity. The original and still dominating PV technology is single-crystal silicon, produced and doped in conventional electronics fabrication techniques. A doped wafer has metalized grid contacts applied to the top surface, with a trade-off between active area shading and charge collection efficiency. Cells are protected with a tempered low-iron cover plate. To reduce reflection of the incoming solar light, textured silicon surfaces and antireflection coatings are used. Commercial cells with this basic design convert ∼17% of the incident energy in sunlight into electricity.[1] Present laboratory cells show over 23% efficiency under terrestrial sunlight.[2]

Textured surfaces are produced by anisotropic etching of the silicon with dilute NaOH solutions. Since certain planes within the crystal are exposed, this process etches silicon much more rapidly in one direction through the crystal structure than another. The appearance of the textured silicon surface is an array of square-based pyramids formed by the intersection of these crystal planes. The silicon surface for textured cells is normally aligned parallel to a (100) plane, and the pyramids are formed by the intersection of (111) planes. The angles of the pyramids are defined by the orientation of the crystal planes. These are such that incident light has at least two chances of being coupled into the cell. If 33% of the incomming light is reflected at each point of incidence, as is the case for normal incidence on bare silicon, then the total reflected light is reduced to 0.33 × 0.33, about 11%.

A further reduction of the reflected light is achieved by using antireflection (AR) coatings, based on the principle of quarter wavelength interference. The fraction of the energy in a normally incident beam of light reflected from the surface of a material covered by a transparent film of thickness d is

$$R = \frac{r_1^2 + r_2^2 + 2r_1r_2\cos 2\theta}{1 + r_1^2r_2^2 + 2r_1r_2\cos 2\theta} \tag{1}$$

where r_1 and r_2 are given by

$$r_1 = \frac{n_0 - n_1}{n_0 + n_1} \qquad r_2 = \frac{n_1 - n_2}{n_1 + n_2} \tag{2}$$

and n_0, n_1, and n_2 represent the refractive indexes of air, AR coating, and silicon, respectively. θ is given by

$$\theta = \frac{2\pi n_1 d}{\lambda} \tag{3}$$

where λ is the wavelength of light. When $n_1d = \lambda/4$, the reflectance is minimum,

$$R_{\min} = \left(\frac{n_1^2 - n_0n_2}{n_1^2 + n_0n_2}\right)^2 \tag{4}$$

The product n_1d is the optical thickness of the film. Any film whose optical thickness is $\lambda/4$ is known as a quarter wave layer. $R_{\min}$ is zero if the refractive index of the AR coating is the geometric mean of those of the materials on either side ($n_1^2 = n_0n_2$). For a silicon cell in air ($n_{Si} \sim 3.8$), the optimum refractive index is the square root of that of Si ($n_{opt} \sim 1.9$). However, since cells are normally encapsulated under glass ($n_0 \sim 1.5$), this increases the optimum value of n_1 to about 2.3. As the refractive

[†] Department of Analytical Chemistry.
[‡] Department of Chemical Engineering.

(1) Rittner, E. S.; Arndt, R. A. *J. Appl. Phys.* **1976**, *47*, 2999−3002.
(2) Green, M. A. *Semicond. Sci. Technol.* **1993**, *8*, 1−12.

0003-2700/96/0368-1095$12.00/0

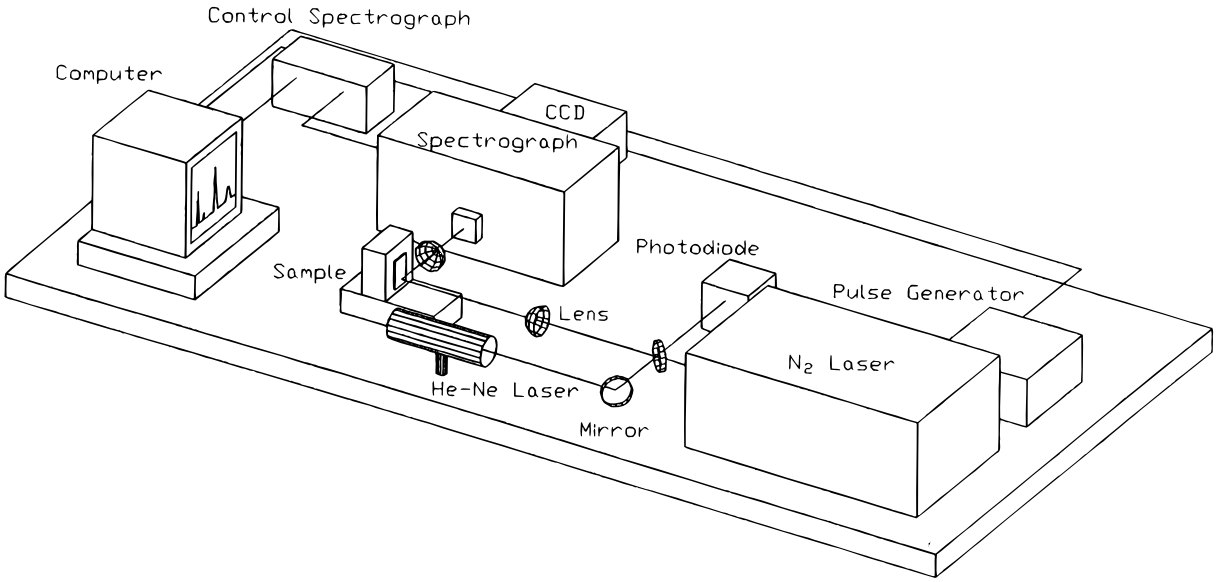

Figure 1. Schematic diagram of the system used for LIBS studies in photovoltaic cells.

index of titanium dioxide is about 2.3, this material is frequently used as an AR coating. With a quarter wave antireflection coating, reflection of sunlight can be kept well below 3%, increasing the output current of the cell by 35−45%.[3]

TiO_2 thin films are thus critical components of photovoltaic cells, and for proper device function, their thickness must be carefully controlled. Rapid and efficient quality control techniques are needed for characterization of these films. Techniques such as ellipsometry are very mature and are used routinely to characterize optical constants and thickness of thin films. The accuracy of thickness measurements is ±0.5 nm, with sensitivity on the order of 0.1 nm. Although a flat, polished solid surface is required, measured films may be solid, liquid, or gas. Ellipsometry, however, provides no information on the chemical composition of the surface.

The laser spark has been used as an excitation source for the analysis of gases, solids, aerosols, and liquids via atomic emission spectroscopy (AES).[4−6] In this method, termed laser-induced breakdown spectroscopy (LIBS), a powerful laser pulse is focused on or in the material to be analyzed. As a result, the material is vaporized and a plasma of high temperature and high electron density is formed, consisting of ions, electrons, and electronically excited atoms. The plasma light can be analyzed spectrally and temporally to determine emitting species.[7−11] LIBS is also suitable for depth profiling. If several laser pulses are allowed to interact with a target, and each laser plasma is analyzed, then a depth profile of the successive layers ablated by the laser is created. Changes in layer composition are indicated by changes in the detected spectral pattern.[12−14]

In this paper, the study of the plasma formed by the interaction of a focused laser beam of wavelength 337.1 nm with TiO_2 coatings of solar cells is described. This study involves an analysis of depth profilings from titanium dioxide layers in solar cells.

EXPERIMENTAL SECTION

A schematic diagram of the system is shown in Figure 1. A pulsed nitrogen laser (Laser Photonics, Model UV-12, wavelength 337.1 nm, pulse duration 10 ns) was used to irradiate solids samples at room temperature in air at 760 Torr. The pulse energy was 1 mJ, of which we estimate only 40% reached the sample. Unless otherwise estated, the central part of the laser beam was isolated with a 6-mm-diameter iris diaphragm and focused onto the sample surface at normal incidence with a quartz planoconvex lens with a focal length of $f = 45$ mm and an f-number of 1.5. The target is placed on a support which is fixed on a bidimensional translation system. To keep irradiation conditions constant, the target is moved perpendicularly to the beam after each data acquisition, unless otherwise noted. The lens−target distance was kept constant during all measurements to $d = f - 5$ mm $= 40$ mm. The laser-ablated plasma emission was collected onto the entrance slit of a triple indexable grating spectrograph (Acton Research Corp., Model SpectraPro 275, Czerny-Turner; $f/3.8$), fitted with classically ruled gratings of 300, 600, and 1800 grooves/mm, blazed at 500 nm. The plasma axis was perpendicular to the spectrograph entrance slit. Optical collection was performed with a glass biconvex lens with a focal length of $f = 35$ mm and an f-number of 1.4. The reciprocal linear dispersion of the spectrometer is 12 nm/mm, with the 300 grooves/mm grating, giving a spectral coverage of 116.4 nm for the detector used. The spectrometer entrance slit was 15 mm high and 20 μm wide. The

(3) Green, M. A. *Solar Cells*; Prentice-Hall: Englewood Cliffs, NJ, 1986.
(4) Radziemski, J. L.; Cremers, D. A. In *Laser-Induced Plasmas and Applications*; Radziemski, L. J., Cremers, D. A., Eds.; Marcel Dekker, Inc.: New York, 1989; pp 295−325.
(5) Moenke, L., Ed. *Laser Microanalysis*; John Wiley & Sons, Inc: New York, 1989.
(6) Aragon, C.; Aguilera, J. A.; Campos, J. *Appl. Spectrosc.* **1993**, *47*, 606−608.
(7) Kim, Y. W. In *Laser-Induced Plasmas and Applications*; Radziemski, J. L., Cremers, D. A., Eds.; Marcel Dekker, Inc.: New York, 1989; pp 327−346.
(8) Laserna, J. J.; Calvo, N.; Cabalin, L. M. *Anal. Chim. Acta* **1993**, *289*, 113−120.
(9) Lee, Y. I.; Sawan, S. P.; Thiem, T. L.; Teng, Y. Y.; Sneddon, Y. *Appl. Spectrosc.* **1992**, *46*, 436−441.
(10) Lee, Y. I.; Thiem, T. L.; Kim, G. H.; Teng, Y. Y.; Sneddom, J. *Appl. Spectrosc.* **1992**, *46*, 1597−1604.
(11) Sdorra, W.; Niemax, K. *Spectrochim. Acta* **1990**, *45B*, 917−926.
(12) Lorenzen, C. L.; Carlhoff; C. Hahn; U. Jogwich, M. *J. Anal. At. Spectrom.* **1992**, *7*, 1029−1035.
(13) Anderson, D. R.; McLeod, W. *J. Anal. At. Spectrom.* **1994**, *9*, 67−72.
(14) Anderson, D. R.; McLeod, W. C.; English, T.; Smith, A. T. *Appl. Spectrosc.* **1995**, *49*, 691−701.

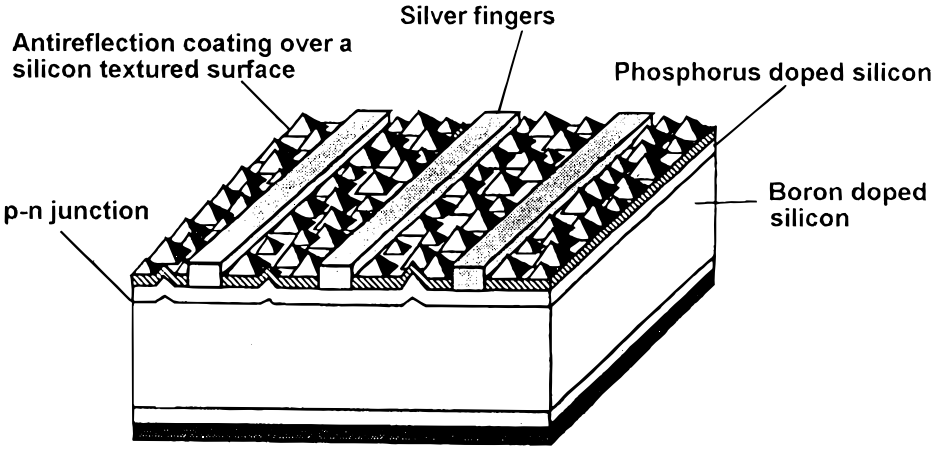

Figure 2. Schematic representation of the elementary design of silicon solar cells.

solid sample was placed ~12 cm from the collection lens, with the distance from the entrance slit to the lens being 5 cm. Thus, the optical magnification was ~0.4. A solid-state two-dimensional charge-coupled device (CCD, EG&G PAR, Thomson CSF, THX-31159A) was used to detect the plasma image. The CCD consists of 512 × 512 elements, each 19 μm × 19 μm. The active area is 9.7 mm × 9.7 mm. This CCD system has a quantum efficiency of 27% at 500 nm. The CCD was cooled to −60 °C by a Peltier system. When cooled to −60 °C, this detector exhibits a dark current of 10 photoelectrons pixel^{-1} s^{-1} and a readout noise of 4−5 electrons/scan. Calibration of the detector system was conducted with a mercury pen lamp. For data adquisition, the CCD system was controled by a pulse generator (Hewlett Packard, Model 4004A), which was optically triggered with a beam deflected from the ablation laser and a fast photodiode. The image of the plasma was then integrated using an acquisition time of 100 ms. Operation of the detector was controlled by a personal computer with OMA Spec 4000 software. The spectrometer is connected to the controlling PC by a conventional IEEE-488 general-purpose interface bus (GPIB). Photovoltaic cells were provided by Isofotón, S.A. (Málaga, Spain) and had the structure shown in Figure 2. Silicon wafers were textured in order to decrease their reflectivity. TiO_2 coatings were grown epitaxially onto the silicon wafers by chemical vapor deposition. Different layer thicknesses were prepared by depositing succesive 40-nm-thick layers onto the substrate.[15] The thicknesses of the TiO_2 films were measured by ellipsometry. Reflectance measurements of solar cell were performed by diffuse reflectance spectrophotometry on a UV−visible difuse reflectance spectrophotometer (Shimadzu, Model MPC-3100).

RESULTS AND DISCUSSION

Figure 3 shows the time-integrated emission spectrum corresponding to a single laser shot of 11 J cm^{-2}. Because of the geometry used here, the plasma axis was parallel to the surface of the spectrograph entrance slit and perpendicular to the slit dimension. The spectrum was taken at a distance of 0.5 mm from the cell surface. For comparison purposes, the background signal corresponding to the dark signal is also shown. The acquisition mode used complete binning of the CCD, with the 512 pixels in the vertical direction (the slit dimension) being summed. A large number of Ti lines are observed, most of them corresponding to

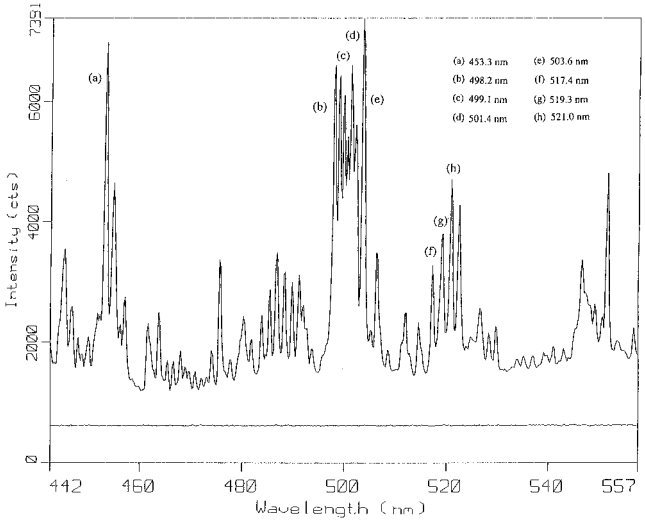

Figure 3. Time-integrated emission spectrum corresponding to a single laser shot of 11 J cm^{-2} onto TiO_2 antireflection coating showing (top) the most intense TiO_2 emission lines and (bottom) background signal corresponding to the dark signal.

Ti(I). The spectral window between 442 and 557 nm provides the most intense Ti lines, and it was used for most experiments. With the present CCD detector, time-integrated intensities are measured, and thus it is not possible to comment on the time evolution of the several lines at various stages in the plasma lifetime. Although the plasma is formed at atmospheric pressure, the laser fluence used is below the threshold for breakdown of air, and hence no lines corresponding to its several components are observed.

Figure 4 shows scanning electron micrographs of the photovoltaic cell surface coated with an epitaxial layer of TiO_2 (160 nm thick). Micrographs A and B were taken respectively after 4 and 15 cumulative laser shots in the same surface area at a fluence of 8.6 J cm^{-2}. Because of the laser beam characteristics, the ablated area shows an elliptical form, with roughly 160 and 40 μm for the dimensions of the long and short axes, respectively. No attempts were made to improve the laser beam profile.

As shown, the cell surface is characterized by an array of silicon pyramids of different size. The TiO_2 coating is not visible since titanium is transparent under the experimental conditions used to scanning electron microscopy. Consequently, the appearance of the silicon pyramids was identical irrespective of the thickness

(15) Cabello, S.; Ruiz, J. *Rev. Ing. Quim.* **1992**, 211−216.

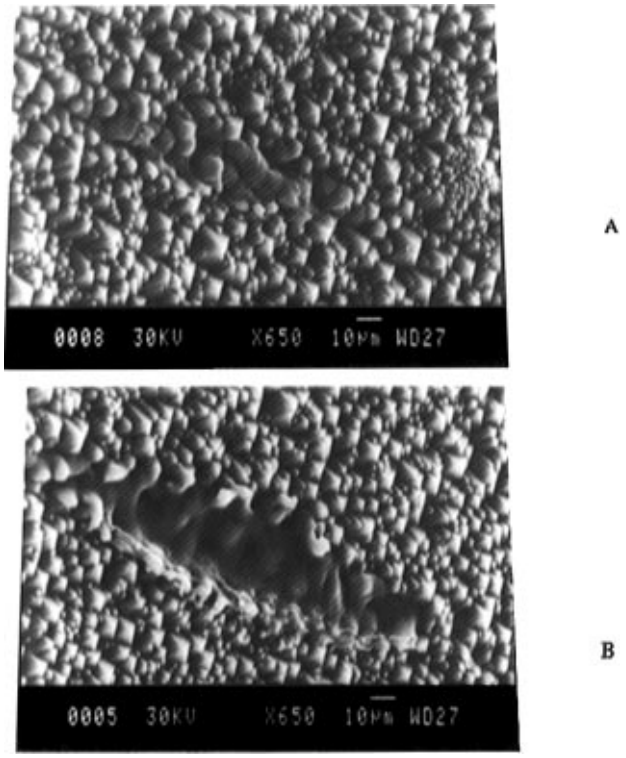

Figure 4. Scanning electron micrographs of the photovoltaic cell surface coated with an 160-nm-thick layer of TiO_2 (A) after four cumulative laser shots and (B) after 15 cumulative laser shots.

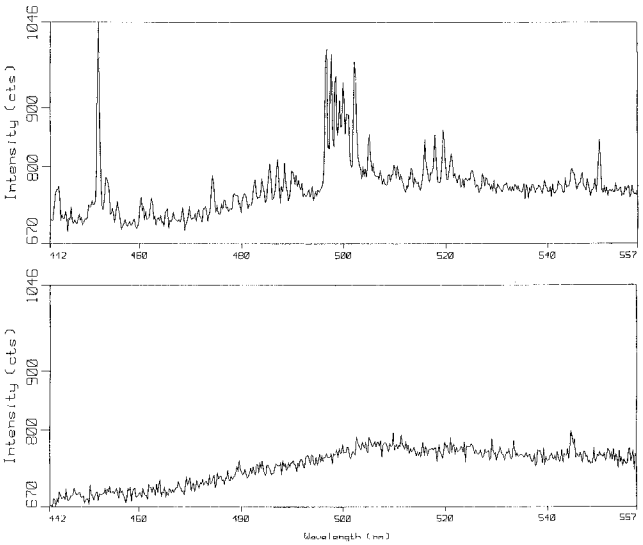

Figure 5. Single-pulse emission spectra corresponding (top) to the fourth laser shot and (bottom) to the fifteenth laser shot onto the solar cell surface correlating with the electron micrographs in Figure 4.

of the TiO_2 coating. As expected, the laser causes melting and vaporization of silicon and, of course, of TiO_2. It should be noted that ablation starts on the vertexes of the pyramids (see bottom right corner of Figure 4A). Subsequent laser pulses ablate deeper layers.

Figure 5 shows single-pulse emission spectra corresponding to the fourth and fifteenth laser shots. The data correlate with the electron micrographs in Figure 4. As shown, after four laser shots, titanium is still clearly distinguishable from the background noise. After 15 laser shots, it is apparent that no TiO_2 is left, and the emission spectrum is characterized only by background noise. Although silicon is being ablated, as evidenced by the audible

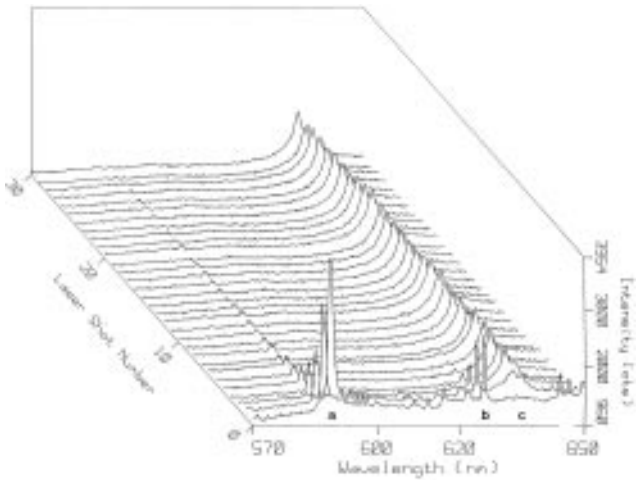

Figure 6. Complete sequence of LIBS spectra showing the photovoltaic cell depth profiling after 30 laser shots on the same surface area. C(I), 589.0 nm (a); Ti(I), 625.9 nm (b); Si(I), 634.7 nm (c).

shock wave, it shows no intense emission lines in the spectral region observed. The effect of further laser pulses is merely to ablate more and more silicon, with no additional spectral information.

The capability of the LIBS technique to provide information on the chemical composition of coated substrates is well illustrated in Figure 6. This set of spectra was performed by choosing a spectral window between 570 and 650 nm in order to monitor both Ti and Si lines of similar emission intensities. As shown, whereas C and Ti signals were present for the first laser shot, no emission of Si was obtained, which means that more than one laser shot is needed to penetrate through the TiO_2 coating. Si emission started for the second laser shot and increased during the ablation process of the coating, after which it became constant, indicating that the coating was completely removed. This is also indicated by the extinction of the Ti line for the fifth laser shot. Behavior similar to that of titanium evolution was displayed by C emission, which is found as an impurity resulting from the solar cells production process. Carbon signal remained longer than titanium signal, since it is present in both AR coating and silicon substrate. Nevertheless, carbon emission decreased because its concentration decreased with depth within the solar cell.

MEASURING FILM THICKNESS USING LIBS

In principle, a straightforward method of measuring film thickness using LIBS could be to acquire a single-laser-shot spectrum and correlate the Ti emission intensity with film thickness. Apart from topographical considerations concerning the silicon substrate, which are important to take into account, this method would be valid if thermal effects alone were responsible for the ablation process. However, with UV laser ablation as used here, the optical constants of the substrate at the laser wavelength contribute definitely to the observed ablation rate and LIBS.

Figure 7A shows the variation of the titanium spectral intensity at 503.6 nm versus coating thickness. The data correspond to single-laser-pulse emission on fresh surfaces. Figure 7B shows

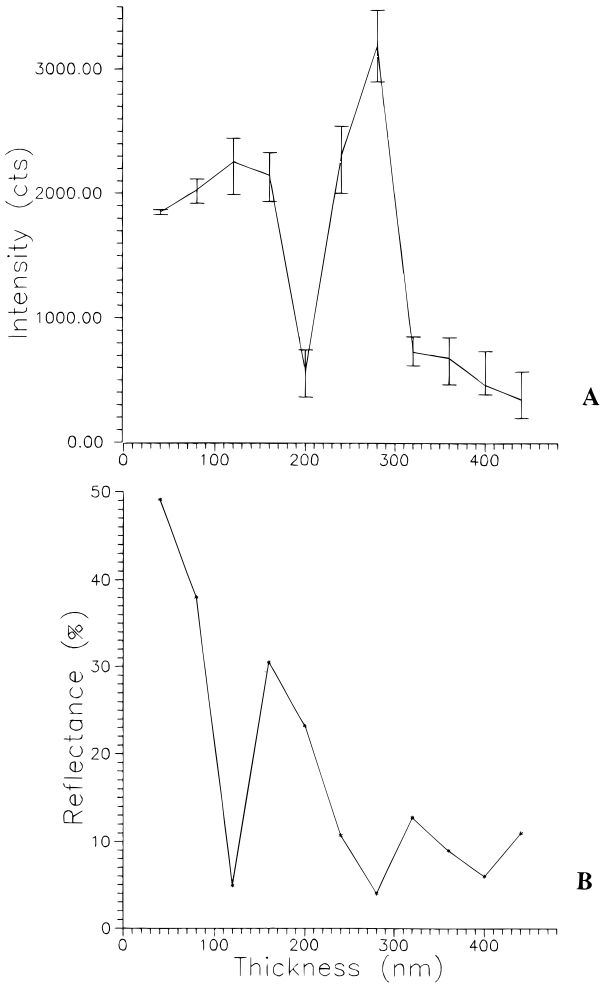

Figure 7. (A) Correlation between spectral intensity at 503.6 nm for the first laser pulse on the surfaces. (B) Variation in substrate reflectivity at laser wavelength (337.1 nm) for different TiO_2 coatings.

the variation of bulk substrate reflectivity at the laser wavelength (337.1 nm) with thickness. Different layer thickness were prepared by depositing several 40-nm TiO_2 layers onto the silicon wafer. As shown there is a fair correlation between spectral intensity and reflectance. Reflectance values follow the harmonic behavior predicted by eq 1. When the coating thickness is such that a minimum in reflectance is observed (at 120 and 280 nm, Figure 7B), the spectral intensity reaches a maximum (Figure 7A). On the contrary, as the reflectance increases, i.e., absorption of laser light decreases, the intensity also decreases. At thicknesses larger than about 350 nm, the correlation is less apparent since the optical behavior of the TiO_2 coating tends to be not well defined. The effect of thickness on the spectral intensity of successive laser pulses is shown in Figure 8. As shown, the behavior of the successive pulses is entirely different of that of the first pulse. Since the surface morphology after the first laser pulse has been destroyed, an optically undefined surface is found, and the ablation depends no longer on the optical behavior of the surface. The result is that the variation of intensity with the laser shot number shows an unexpected dependence. These results confirm the significance of the optical factor on the ablation behavior of samples absorbing at the laser wavelength. Also, the results reveal that a simple relationship between LIBS intensity and thickness cannot be established.

An alternative method to measure coating thickness is to determine the cumulative dose or total laser energy in joules

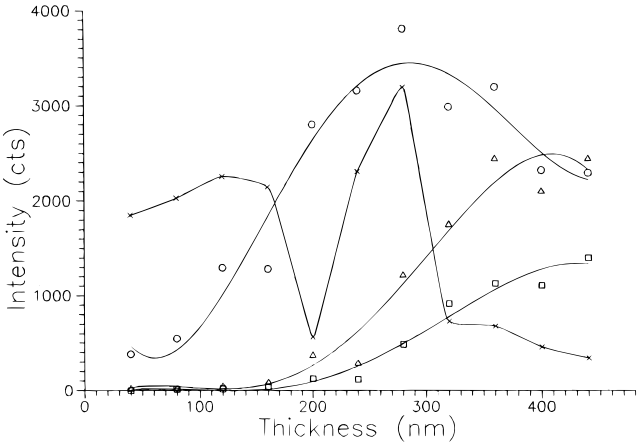

Figure 8. Emission intensity variation versus TiO_2 coating thickness for different laser pulses on the cell surface. x, Pulse 1; ○, pulse 2; △, pulse 3; and □, pulse 4.

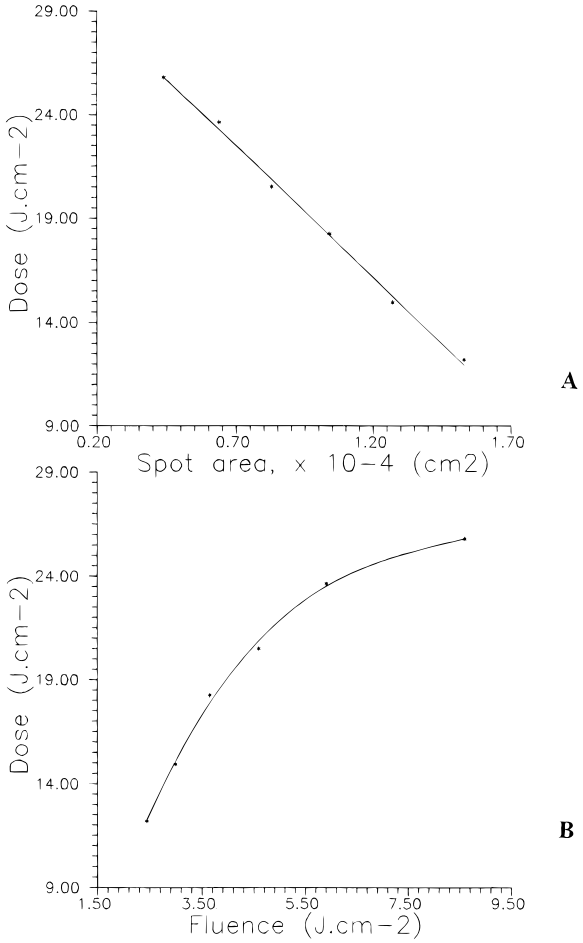

Figure 9. Dose needed to deplete a 40-nm-thick TiO_2 layer versus (A) ablated surface and (B) laser fluence.

needed to ablate completely the TiO_2 coating. We assume that the film was totally depleted when the peak height of the Ti line at 503.6 nm was twice the peak-to-peak noise of the spectrum. For a given thickness, the depleting dose will depend on the laser fluence and the angle of incidence. Since no direct control on the pulse energy is available with the present laser, the laser beam diameter was changed by moving the sample position relative to the laser focal point, as a mean of modifying the laser fluence. Figure 9, parts A and B, show the depleting dose for a 40-nm-thick TiO_2 film as a function of ablated surface area and fluence,

respectively. As shown, the depleting dose increases at larger laser spot area or, in other words, at low fluence. The number of laser shots needed to deplete completely the film is larger as the fluence decreases. Working at low laser fluence results in ablation of a larger surface area and less lateral resolution. In addition, since spectral information derives from single-laser-shot measurements, the spectral signal-to-noise ratio deteriorates at low fluence, causing poorer precision in the estimation of the depleting dose. At 8.6 J cm^{-2}, the ablated surface area is $\sim 4 \times 10^{-5}$ cm^{-2}, which corresponds to an ablated elliptical profile with semiaxes of 85 and 15 μm. This fluence was used for further measurements using normal incidence. The relationship obtained between depleting dose and film thickness shows linear response between 40 and 400 nm (1 and 10 layers) of TiO_2. This range is within the typical values used in solar cells. For instance, depletion of a 320-nm layer would require under the present experimental conditions 0.0035 J. This depleting dose can be supplied in the form of 10 pulses at 8.6 J cm^{-2}.

CONCLUSIONS

Although pulsed-laser ablation by infrared and visible lasers is considered to be based on purely thermal mechanisms, the situation is different for UV laser ablation. We point out the important role of the substrate optical constants for the plasma formation and subsequent spectral measurements. The sensitivity of the present method for thickness measurements is limited. Sensitivity can be increased by decreasing the laser fluence. This would result in a larger number of laser shots needed to ablate a given thickness and, thus, a better capability to distinguish thickness differences. The limit to which the fluence can be decreased is, in this case, the ablation threshold, which for TiO_2 films using our instrumental configuration is about 1 J cm^{-2}. The range of thicknesses which can be studied is between 40 and 400 nm, within the typical values used in solar cells.

Received for review October 5, 1995. Accepted January 10, 1996.[⊗]

AC951002I

[⊗] Abstract published in *Advance ACS Abstracts,* February 15, 1996.